RAPID COMMUNICATIONS

PHYSICAL REVIEW E VOLUME 52, NUMBER 5 NOVEMBER 1995

Competing patterns in the Faraday experiment

Krishna Kumar* and Kapil M. S. Bajaj†
Department of Physics, Indian Institute of Technology, Kanpur 208 016, India
(Received 27 June 1994)

Competition between subharmonically generated equilateral triangles and regular hexagons is observed in the Faraday experiment with viscous fluids subjected to a sinusoidal forcing. For kinematic viscosities around 17 cm^2/s, all spatially regular patterns—stripes, squares, hexagons, and triangles can be parametrically excited in the same fluid depending on the forcing amplitude and frequency. Close to this value of viscosity, hexagonal and square patterns coexist showing a bicritical point.

PACS number(s): 47.35.+i, 47.20.Ky, 61.43.−j

The generation of standing waves on a free surface of a horizontal layer of fluid subjected to vertical oscillation, known since the observations of Faraday [1], provides the simplest experimental model of parametric excitation in spatially extended dissipative systems. It is also an equally interesting system to study pattern forming instabilities with only two control parameters—the oscillation amplitude and the frequency of vibration. Recent studies on viscous fluids [2,3] have opened up a rich field for investigating pattern selection in dissipative systems. These experiments involve two-frequency forcing [2,3] and show a variety of patterns: stripes, squares, hexagons, triangles, and twelvefold quasicrystalline structure [2], depending upon the forcing amplitude, and the ratio of and the phase between the imposed frequencies. However, in the original version of the Faraday experiment, i.e., with sinusoidal forcing, stripes [2,4] in high viscosity fluids and squares [5] in low viscosity fluids are the only regular patterns observed. The linear stability analysis [6] for a thin layer of viscous fluid shows that the selection of the critical wave number is strongly influenced by the presence of large dissipation in the Faraday experiments. We report on competing hexagonal and triangular patterns and the observation of a bicritical point, where fourfold and sixfold patterns coexist, in the Faraday experiment with a *single* frequency sinusoidal forcing. We clearly demonstrate the importance of the role of viscosity on pattern selection by Fauve *et al.* [7] in a liquid-vapor system.

Experiments reported here are performed using an electromagnetic shaker (VS3202, IMV Japan), which provides a clean vertical vibration over a wide range of frequencies (5–5000 Hz). The shaker is mounted on a pneumatic suspension base for vibration isolation. The horizontal component of the acceleration is less than 1.3% of the vertical component over the frequency range (20–200 Hz) used in this experiment. The shaker is excited at a frequency of $\omega/2\pi$ using a power amplifier (VA-ST-0.3, IMV Japan) which is in turn fed with a pure sinusoidal oscillator (distortion <-55 dBc) from a function generator (HP 3314A) with a frequency accuracy of better than $\pm 0.6\%$ and an amplitude accuracy of $\pm 1\%$. Acceleration is measured using a light weight piezoelectric accelerometer (B&K 4374) and a charge amplifier (B&K 2635). The charge amplifier output is Fourier transformed on a spectrum analyzer (HP 3582A) to obtain the acceleration amplitude a, at the excitation frequency.

We have used cylindrical containers of circular cross section (diameter 81–143 mm, depths 1.5–6.0 mm) and a square container (140 mm side, 4 mm depth). Precise measurement have been made on fluids in an 81 mm diameter circular cross section and square containers made out of plexiglass. The brimful technique [8] has been used in all the measurements to minimize the meniscus effects. Experiments on various mixtures of glycerol and water with mass fractions of glycerol in the range 65%–87 % have been performed at a temperature of 29.0 ± 0.5 °C. We use a relatively thin layer of fluid to suppress the large wavelength ($k\to 0$) perturbations. The containers are covered with a transparent plastic sheet to minimize evaporation of water and contamination of the surface. The patterns are observed with a stroboscope (GR 1538A) set at frequencies $\omega/2\pi n$, where n is an integer. For fluids with kinematic viscosity $\nu\approx 17\times 10^{-2}$ cm^2/sec the selection of patterns is quite interesting. In less viscous fluids we observe only squares and lines are observed in fluids with much higher viscosity. We report in this paper our observations for $\nu=17\pm 0.2\times 10^{-2}$ cm^2/sec.

Our experiments differ from those on low viscosity fluids [5] due to relatively large dissipation chosen and from that of Müller [3] in terms of the forcing function which has important consequences for the symmetries of the nonlinear stability problem. In general, in a spatially extended system, the surface deformation $\zeta(\mathbf{r},t)$ just above the instability onset a_c may be expressed as

$$\zeta(\mathbf{r},t)=\left(\sum_{j=1}^{N} A_j(T)\exp(i\mathbf{k}_j\cdot\mathbf{r})+\text{c.c.}\right)\zeta(t)e^{i\alpha t}+\cdots, \qquad (1)$$

where $\mathbf{k}_j$ and A_j are the horizontal wave vector and the complex amplitude, respectively, of the jth standing wave, $i\alpha$ is the Floquet exponent, and T is a slow time scale of $O(1/\epsilon)$ where $\epsilon\equiv a/a_c-1$. The threshold a_c is, in general, a complicated function k, ω, ν, fluid depth h, and other fluid parameters [6]. For given fluid parameters, a_c increases with increasing ν and/or increasing ω. The time-periodic function $\zeta(t)$ has a period $2\pi/\omega$.

As the effect of external forcing is equivalent to gravity modulation, we have an instance of parametric forcing in our experiment. For sinusoidal forcing f_1 given by

*Permanent address: Physics and Applied Mathematics Unit, Indian Statistical Institute, 203, B T Road, Calcutta 700 035, India.
†Present address: Department of Physics and Center for Nonlinear Science, University of California, Santa Barbara, CA 93106.

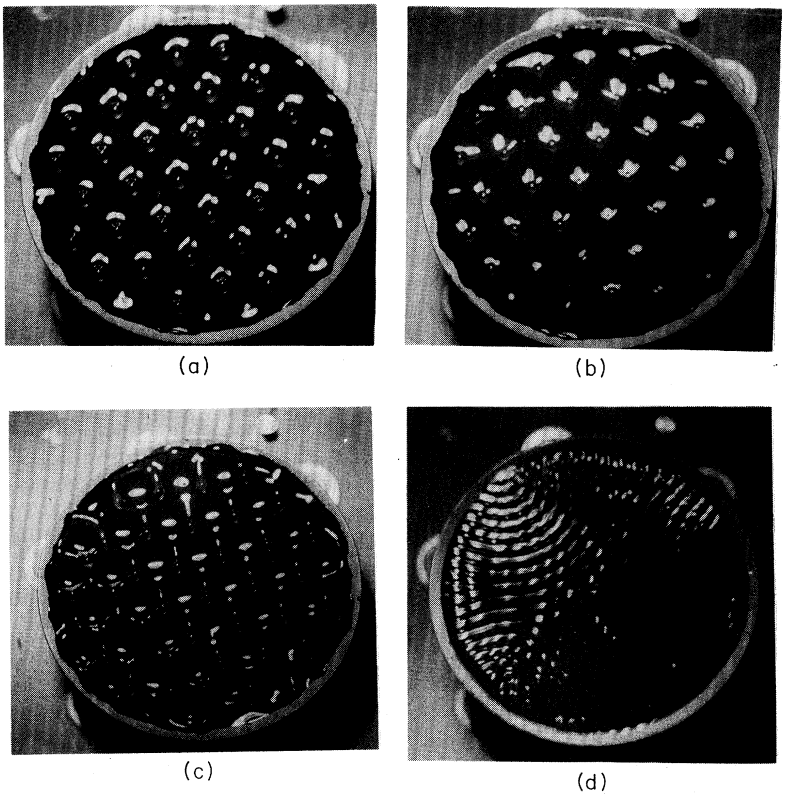

FIG. 1. Photographs of subharmonically generated nonlinear patterns in a circular container (81 mm diameter) oscillating at 40 Hz: (a) hexagons ($\Phi=0$); (b) equilateral triangles ($\Phi\approx\pi/2$); (c) hexagons ($\Phi\approx\pi$) with reversed fluid flow directions; (d) stripes (at 180 Hz and much above the onset). The strobe light illumination is at near-grazing angle, and the camera is axis symmetric with the oscillation. The white patches are reflections from curved fluid surfaces. Fluid parameters: $h=2$ mm and $\nu=17.0\pm0.2\times10^{-2}$ cm^2/s.

$$f_1(t)=a\cos(\omega t), \tag{2}$$

we have $f_1(t+\pi/\omega)=-f_1(t)$. The most efficiently amplified response then pulsates at frequency $\omega/2$ as first noticed by Faraday [1]. The Floquet multiplier $\Lambda=e^{2\pi i\alpha/\omega}$ for this case is -1. It follows that the invariance $t\rightarrow t+2\pi/\omega$ is broken at the instability onset. For a nonzero solution $\zeta(\mathbf{r},t)$ this implies that $\zeta(\mathbf{r},t+2\pi/\omega)=-\zeta(\mathbf{r},t)$ is also a solution. Consequently, the evolution equation for the amplitude A_j should be invariant under the transformation $A_j\rightarrow -A_j$. For two-frequency drive as used in Refs. [2] and [3] the forcing function f_2 is of the type

$$f_2(t)=a[\cos\delta\cos(p\omega t)+\sin\delta\cos(q\omega t+\phi)] \tag{3}$$

with $a\cos\delta(a\sin\delta)$ as the amplitude at frequency $p\omega(q\omega)$, the forcing still has a period $2\pi/\omega$. In Eq. (3) above, p and q are integers. The phase can be varied in the range $[0,2\pi/p]$ since there exists an integer m such that the transformation $\phi\rightarrow\phi+2\pi/p$, $t\rightarrow t+2m\pi/p\omega$ keeps the forcing function $f_2(t)$ invariant. Now, $f_2\ (t+\pi\omega)=f_2$ if both p and q are even and $f_2(t+\pi/\omega)=-f_2(t)$ if both p and q are odd. However, for p and q of different parity this transformation is not valid and the response is amplified most efficiently at frequency ω. The corresponding Floquet multiplier Λ is then $+1$. The invariance $A_j\rightarrow -A_j$ is no longer valid and the evolution equation for the amplitude A_j may involve quadratic (i.e., even order) nonlinearities. Consequently, harmonically oscillating patterns are generated through backward bifurcation. If the coefficients of the resulting quadratic terms in the amplitude equation vanish, the resulting pattern could be subharmonic.

In our case with a sinusoidal forcing given by f_1, we see only subharmonically generated patterns as expected and the bifurcation is forward. In contrast to the earlier observations [3], where sixfold and threefold patterns fluctuate "indifferently," we see periodic behavior. In addition, depending on the forcing frequency and the amplitude, we observe in one single fluid *all* the regular patterns that can be realized in a spatially extended system. The observed patterns tile the free surface completely and are independent of the geometry.

For a fixed external frequency ω the free surface of the fluid is destabilized as the forcing amplitude is raised above a threshold value a_c. The resulting standing waves form different periodic spatiotemporal patterns depending upon the values of ω, a, and ν. Figures 1(a)–1(c) show competition between sixfold and threefold patterns in the circular container vibrating at 40 Hz in a strobe light at half the frequency. These patterns are the nonlinear superpositions of three standing waves of different phases. Figure 1(a) shows a sixfold pattern. The fluid rises on vertices and the center of a regular hexagon. As the cycle progresses, the fluid rises, along the lines joining the vertices and the center which form the equilateral triangles. However, the fluid falls only in three alternate triangles [slightly convex in Fig. 1(b)] and rises in the other three [slightly concave in Fig. 1(b)]. The fluid flow in this figure thus shows a threefold pattern. Next, the fluid begins to rise along the sides of regular hexagons [Fig. 1(c)] constructed by joining the centers of all the triangles of Fig. 1(b), and falls at the centers of newly formed hexagons, i.e., at the vertices of triangles of Fig. 1(b). Thus the regular hexagons of Fig. 1(a) and Fig. 1(c) have fluid flow in opposite phases. These patterns are subharmonically generated slightly above the instability onset and alternate periodically over a time scale that is long compared to the period of imposed vibration. The continuous transitions from hexagons

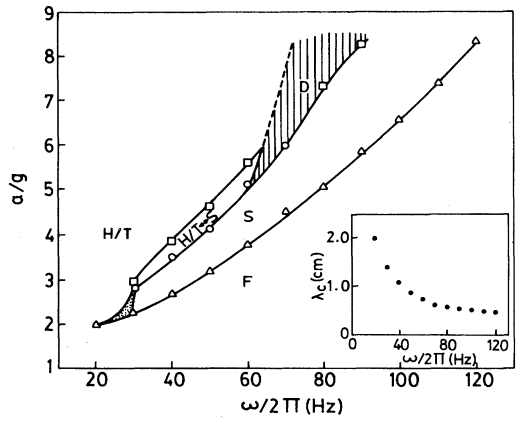

FIG. 2. Bifurcation diagram of various structures in a square cell (140 mm^2, $h=3.6$ mm). The flat surface (F) is destabilized for accelerations above a_c (the lowest curve). At 20 Hz, the patterns at the primary instability are alternating hexagons and triangles (H/T). For $30\leq\omega/2\pi\leq120$ the patterns at the onset are squares (S). The small shaded area is the bicritical region where stable H/T as well as S coexist. In the region ($H/T\leftrightarrow S$) the structures periodically alternate between hexagons, triangles, and squares. Square patterns with hexagonal or triangular defects (both time independent and dependent) are observed in region D. The dashed line (not measured) represents the expected boundary between H/T and D. The inset shows the dispersion relation at the onset.

to equilateral triangles and back take place through various threefold symmetric structures known as triangular patterns [9]. At high frequencies (<120 Hz) squares are generated at the instability onset. At much higher frequencies (≈180 Hz), raising the forcing amplitude much above the onset value results in appearance of stripes [see Fig. 1(d)]. We observe similar behavior in the container with a square cross section.

Figure 2 gives the bifurcation diagram in the parameter space (a,ω) as measured in the square cell. At low frequencies (≈20 Hz), the patterns observed at the instability onset are periodically alternating hexagons (H) and equilateral triangles (T). For frequencies 20 and 30 Hz, alternating hexagons and triangles coexist with square pattern. At higher frequencies (>30 Hz) the pattern at the onset is square. In the frequency range (30–60 Hz), when the forcing amplitude a is raised much above the threshold value a_c, the fourfold patterns bifurcate to periodically alternating threefold and sixfold patterns (see area $H/T\leftrightarrow S$ in Fig. 2). In the area denoted D the appearance of various patterns is chaotic. Figure 3 shows the typical photographs in the square cell. Figure 3(a) shows rhombic structure with angles $2\pi/6$ and $2\pi/3$. This is one of the various possible patterns due to the nonlinear combination of three standing waves with a neutral phason mode. Figure 3(b) shows a slight distortion of a regular hexagonal lattice while Fig. 3(c) shows a square lattice. Figure 3(d) shows a photograph in which hexagonal and square patterns coexist giving rise to a bicritical point slightly above onset. We have observed coexisting square and hexagonal patterns at different relative positions in the same container in different runs. We thus believe that this effect may not be due to inhomogeneity in the forcing.

The periodic behavior of subharmonically generated hexagonal and triangular states can be understood in the framework of amplitude equations. Hexagonal and triangular patterns are closely related because both require three wave vectors of same length. We consider the $N=3$ case in Eq. (1) of complex amplitudes with wave vectors of equal length ($|\mathbf{k}_l|=k_c$) and $\mathbf{k}_1+\mathbf{k}_2+\mathbf{k}_3=0$. Using symmetry arguments

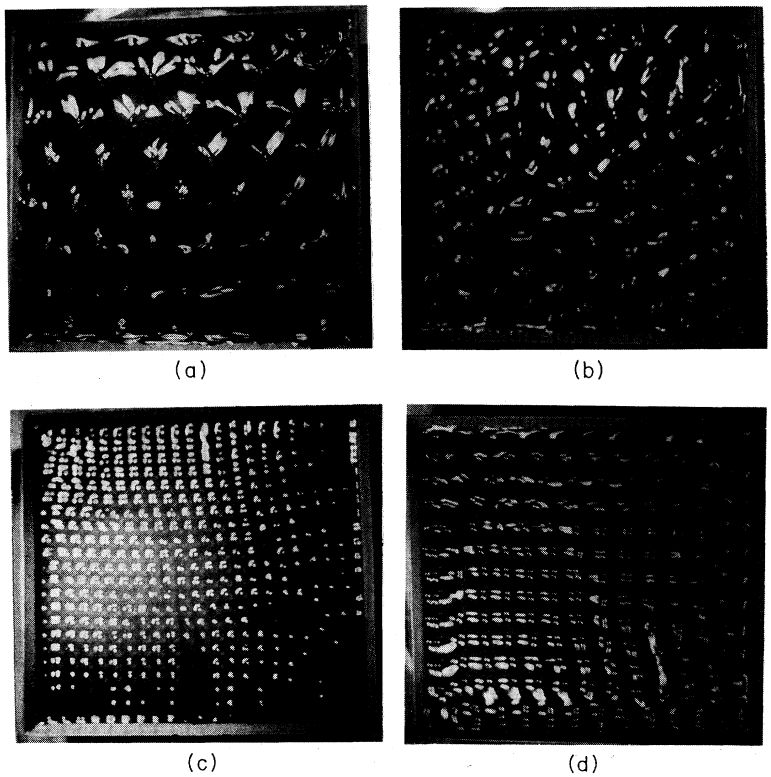

FIG. 3. Typical patterns in the square cell (diameter = 140 mm; $h=2.6$ mm): (a) rhombic structure (angles $2\pi/6$ and $2\pi/3$) at 20 Hz; (b) hexagons at 30 Hz; (c) squares at 80 Hz; (d) bicritical point—existence of squares and hexagons or triangles at 40 Hz.

the relevant part of the evolution equation in amplitudes [10] up to fifth order can be written as

$$\partial_T A_l = \epsilon A_l - (\beta_1 A_l A_l^* + \beta_2 A_m A_m^* + \beta_3 A_n A_n^*) A_l - \gamma A_l^* A_m^{*2} A_n^{*2} - O(5) \ldots, \quad (4)$$

where $O(5)$ refers to other fifth order terms that are compatible with the symmetries. Equations for A_m and A_n can be obtained by cyclic permutation of (l,m,n). The invariance of the patterns under space reflection ($\mathbf{r} \rightarrow -\mathbf{r}$) requires that all the coefficients in Eq. (4) should be real.

The linear growth rate ϵ depends on viscosity ν and other fluid parameters through a_c. However, its value can be set externally by fixing the relative distance from the instability onset. The pattern selection is decided by the coefficients β_i of the nonlinear terms in Eq. (4). In the absence of the quintic term (i.e., $\gamma = 0$), hexagonal and triangular structures are degenerate. This degeneracy is lifted if γ is nonzero. The coefficients β_i and γ are, in general, functions of ν, ω, a and other fluid parameters. In the above model, β_i should be positive in order to have saturation of growing amplitudes, while γ may have either sign. The homogeneity and isotropy of the fluid imply $\beta_1 = \beta_2 = \beta_3$. Although the form of the amplitude equation, Eq. (4), is dictated by the symmetry of the problem, the nonlinear coefficients ϵ, β_i, and γ are decided mainly by ν, a, and ω. Thus Eq. (4) holds for less viscous fluids as well as highly viscous fluids but the predicted patterns may not be stable in all fluids. We see hexagonal and triangular patterns at the onset for intermediate range of viscosities for frequencies between 20 and 30 Hz. For relatively higher frequencies ($30 < \omega/2\pi < 60$ Hz) these patterns are observed at much above onset (Fig. 3). One then needs to consider other possible amplitude equations.

The magnitude of all the amplitudes A_l in Eq. (4) must be equal for regular patterns. The complex amplitude A_l, therefore, may be expressed as $A_l = R \exp(i\phi_l)$ for regular patterns. The third term on the right hand side couples phases with real amplitude R. Two of these phases are related by the symmetry of the regular pattern in the horizontal plane. The remaining one is a marginal mode, also known as the phason mode, and can be parametrized by $\Phi = \phi_1 + \phi_2 + \phi_3$. Considering Eq. (4) only up to third order, the equation for this phason is simply

$$\partial_T \Phi = 0. \quad (5)$$

The phase Φ can take any value. Therefore, all the possible states are degenerate. The degeneracy is lifted by the relevant quintic term ($\gamma \neq 0$) of the amplitude equation, and the resulting phase evolves as

$$\partial_T \Phi = 3\gamma R^4 \sin(2\Phi). \quad (6)$$

The equilibrium points of Eq. (6) yield $\Phi = s\pi/2$, where s is an integer. The regular patterns [9] due to three standing waves may be most generally expressed as

$$\zeta(\mathbf{r},t) = \zeta(t)\exp(i\alpha t)[\cos(\mathbf{k}_1 \cdot \mathbf{r} + \phi_1) + \cos(\mathbf{k}_2 \cdot \mathbf{r} + \phi_2) + \cos(\mathbf{k}_3 \cdot \mathbf{r} + \phi_3)]R/3, \quad (7)$$

where the three wave vectors are defined as $\mathbf{k_1} = k_c \hat{e}_x$, $\mathbf{k_2} = -(\hat{e}_x - \sqrt{3}\hat{e}_y)k_c/2$, and $\mathbf{k_3} = -(\hat{e}_x + \sqrt{3}\hat{e}_y)k_c/2$. If θ is the angle between the direction of $\mathbf{k_1}$ and position vector $\mathbf{r}$, Eq. (7) remains invariant under the transformation $\theta \rightarrow \theta + \pi/3$ when ϕ_i are even multiples of $\pi/2$. Similarly, it is invariant under the transformation $\theta \rightarrow \theta + 2\pi/3$, if ϕ_i are odd multiples of $\pi/2$. That is, for even s, the resulting patterns are sixfold (hexagonal H), and for odd s the patterns are threefold (equilateral triangles T).

Stability analysis of these two fixed points using Eq. (6) shows that the state $H(T)$ is weakly stable if γ is negative (positive) and the growth rate of phase perturbation is proportional to R^4. This implies that the system would settle in one of the H or T states after a long time. However, the lateral walls which break the symmetries of an infinite plane may cause both the states to become weakly unstable. This may be the reason for the observed periodic behavior.

In this paper, we have reported a periodic competition between subharmonically generated hexagons and equilateral triangles in a viscous fluid. The phason mode Φ changes periodically leading to competing sixfold and threefold patterns. In a fluid with kinematic viscosity $17 \pm 0.2 \times 10^{-2}$ cm^2/sec hexagons and squares coexist at the onset leading to the possibility of a bicritical point in the Faraday experiment. In this range of viscosity, all possible regular patterns can be generated subharmonically in a single fluid by varying the amplitude and the frequency of the external forcing.

We thank J. K. Bhattacharjee and R. Mehrotra for a critical reading of the manuscript and fruitful suggestions. We benefited from discussions with A. K. Mallick, A. K. Majumdar, B. Ravindra, and S. N. Gossain. This work was supported by Department of Science and Technology, India.

[1] M. Faraday, Philos. Trans. R. Soc. London Ser. A **52**, 299 (1831).

[2] W. S. Edwards and S. Fauve, Phys. Rev. E **47**, R788 (1993); C. R. Acad. Sci. (Paris) **315-II**, 417 (1992).

[3] H. W. Müller, Phys. Rev. Lett. **71**, 3287 (1993).

[4] W. S. Edwards *et al.* (unpublished).

[5] A. B. Ezerskii *et al.* [JETP Lett. **41**, 157 (1986)], Pis'ma Zh. Éksp. Teor. **41**, 129 (1985); N. Tufillaro *et al.* Phys. Rev. Lett. **62**, 422 (1989); S. Douady, J. Fluid Mech. **221**, 383 (1990); S. Cilliberto *et al.* Europhys. Lett. **15**, 23 (1991).

[6] K. Kumar, Proc. R. Soc. London Ser. A (to be published); K. Kumar and L. S. Tuckerman, J. Fluid Mech. **279**, 49 (1994).

[7] S. Fauve *et al.* Phys. Rev. Lett. **68**, 3160 (1992).

[8] T. B. Benjamin and C. Scott, J. Fluid Mech. **92**, 241 (1979).

[9] M. Golubitisky *et al.* Physica **10D**, 249 (1984).

[10] M. C. Cross and P. C. Hohenberg, Rev. Mod. Phys. **65**, 851 (1993).

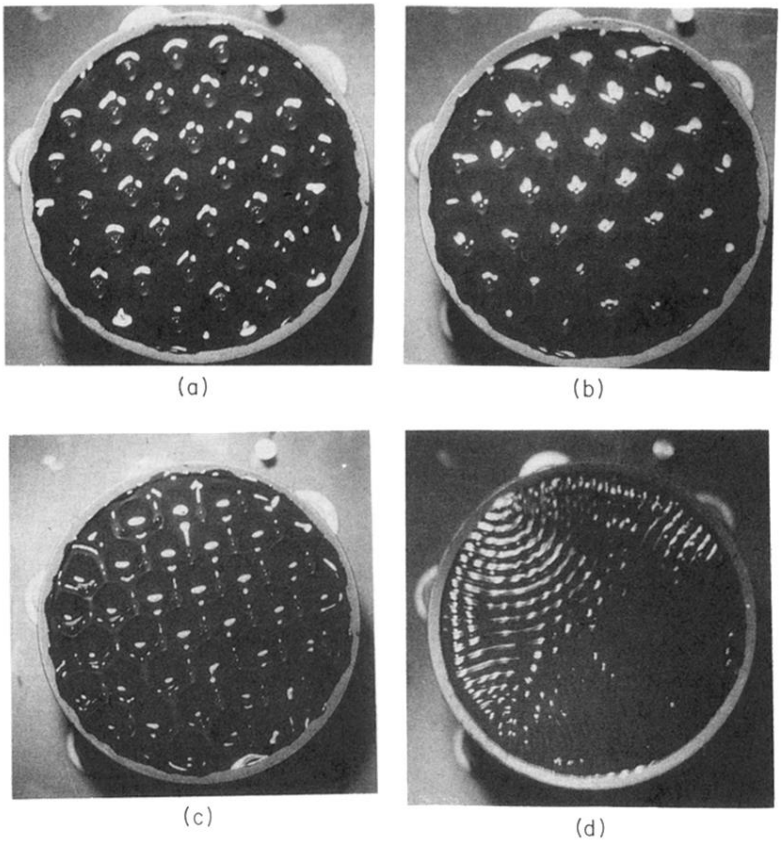

FIG. 1. Photographs of subharmonically generated nonlinear patterns in a circular container (81 mm diameter) oscillating at 40 Hz: (a) hexagons ($\Phi=0$); (b) equilateral triangles ($\Phi\approx\pi/2$); (c) hexagons ($\Phi\approx\pi$) with reversed fluid flow directions; (d) stripes (at 180 Hz and much above the onset). The strobe light illumination is at near-grazing angle, and the camera is axis symmetric with the oscillation. The white patches are reflections from curved fluid surfaces. Fluid parameters: $h=2$ mm and $\nu=17.0\pm0.2\times10^{-2}$ cm^2/s.

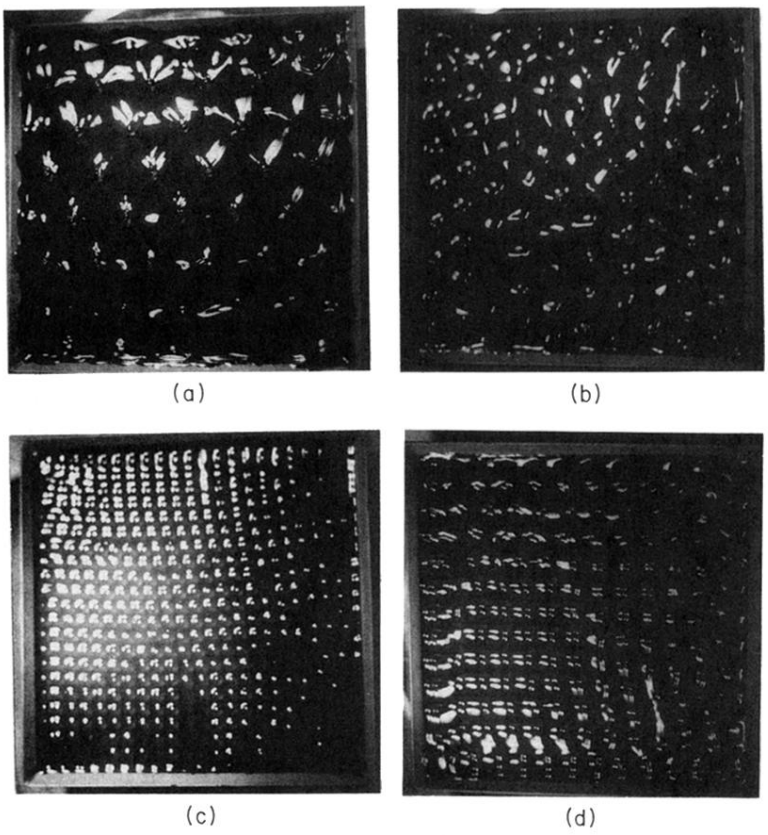

FIG. 3. Typical patterns in the square cell (diameter = 140 mm; $h = 2.6$ mm): (a) rhombic structure (angles $2\pi/6$ and $2\pi/3$) at 20 Hz; (b) hexagons at 30 Hz; (c) squares at 80 Hz; (d) bicritical point—existence of squares and hexagons or triangles at 40 Hz.